Monitoring of Internal Phosphorus Loading, Water Column Mixing, Cyanobacterial Blooms and Dreissenid Mussels In Conesus Lake NY (Summer 2018)

Report Submitted to
The Livingston County Planning Department

By

Isidro Bosch, Michael Chislock+,
Katelynn Warner, Emelyn Bell
and
Karl Hanafin*

Department of Biology
State University of New York at Geneseo

+Department of Environmental Science and Ecology
The College at Brockport

*** York Central School (retired)**

February 15, 2019

TABLE OF CONTENTS

LIST OF TABLES, FIGURES AND APPENDICES

TABLES

FIGURES

APPENDICES

I. SUMMARY

- As part of the Conesus Lake 2018 monitoring program, the primary goal of this research was to measure the magnitude of anoxic internal phosphorus (P) loading in the south and central lake basins and to investigate the relationship between wind-driven water column mixing of P and the onset of cyanobacterial blooms.

- Hypolimnetic TP build up began in late June and presumably continued until turnover, which occurred on Sept. 24, Oct. 17 and Oct. 24 in the north, central and south basins, respectively. TP accumulated at a rate of 38.9 $Kg \cdot day^{-1}$ in the hypolimnion. Near bottom TP concentrations reached maxima of 230 $\mu g \cdot L^{-1}$ in the south basin and 120 $\mu g \cdot L^{-1}$ TP in the central basin. Release rates and concentrations of TP were low compared to 2009, 2014 and 2017, but higher than in 2004.

- The deeper south basin, with a large hypolimnetic volume and higher water column stability/resistance to mixing, is the primary source of internally loaded P into Conesus Lake, followed by the central basin and the shallower north basin.

- High winds led to significant disruptions of water column density stratification, as indicated by temperature data. A wind-aided mixing event on June 28 was followed by a short bloom of colonial cyanobacteria and subsequently by a lake-wide bloom of single-celled cyanobacteria that lasted approximately two weeks. Single cell numbers > 175 x 10^3 mL^{-1} associated with high turbidity (6.5-8.8 NTU) and shallow Secchi depth (0.9-1.2) persisted from July 4-11.

- High winds on July 30 and Aug. 1 again caused mixing of the water column. This event was associated with increases in oxygen saturation and oxidation-reduction potential in the hypolimnion, and with higher TP near the surface. By the 11th and the 15th of August, cyanobacteria abundance had increased to 4.1 colonies$\cdot mL^{-1}$ and 7.1 colonies$\cdot mL^{-1}$ from a low of 0.5 colonies per mL on July 24.

- Although regular monitoring activities were completed on the 23rd of August, we continued sampling through September. Powerful winds on August 21, 29 and Sept. 1 caused mixing of the water column to 12 m. By Sept. 1 another bloom of colonial cyanobacteria was detected. Average chlorophyll a values had increased by 50% to > 12 $\mu g \cdot L^{-1}$. This bloom continued until our last sampling date of the season.

- Detailed analyses of cyanobacteria species composition and biovolume were carried out in from samples collected during the June 28 and September 13. The dominant taxa included *Dolichospermum* and *Gomphosphaeria* sp. on June 28, and *Dolichospermum*, *Microcystis* and *Aphanocaspa* sp. on September 13. The biovolume of cyanobacteria was nearly three times higher in the September bloom than in the June bloom.

- A survey of adult dreissenid mussel populations was conducted. Zebra mussel numbers remain relatively low compared to population numbers recorded during the early years of the invasion. No quagga mussels were counted among the more than 550 mussels inspected in this study.

II. INTRODUCTION

Blooms of potentially toxic cyanobacteria (a type of harmful 'algal' bloom or HAB) pose one of the most serious threats to lake water quality worldwide. Of the many species that contribute to HABs in lakes, *Microcystis aeruginosa* is of greatest concern due to its propensity to form large blooms and to produce chemicals known as microcystins, which, even at low concentrations, may have acute and chronic affects on human health.

Cyanobacterial blooms are not a new type of disturbance, but their frequency in temperate lakes worldwide has increased since the 1990's due to nutrient enrichment and climate warming. In the Great Lakes region, the spread of the invasive zebra mussel, *Dreissena polymorpha,* since the mid 1980's also contributed to surges in cyanobacterial HABs. Zebra mussels selectively feed on non-toxic phytoplankton, such as diatoms and green algae and reject *Microcystis* and other toxic cyanobacteria*,* thus favoring these species in terms of competition for dissolved nutrients (e.g.VanderPloeg *et al*., 2001; Raikow *et al*., 2004). Zebra mussels colonized the Great Lakes system in 1984 and by 1992 they had dispersed into Conesus Lake. In the 1990's the Eurasian quagga mussel (*D. rostriformis bugensis*), colonized North America and supplemented or largely replaced zebra mussels in temperate lakes. Because they feed at similar size-dependent rates and exhibit some of same rejection mechanisms as zebra mussels, quagga mussels are expected to intensify the threat of *Microcystis* and cyanobacterial blooms (Tang et al., 2013). The last survey of mussels in Conesus Lake was conducted in 2013 (Bosch and colleagues, 2013), and no quagga mussels were detected in that study. One of the goals of this summer's monitoring is to determine whether quagga mussels have colonized Conesus Lake since 2013.

Conesus Lake has a history of cyanobacterial blooms that goes back to the 1960's (Mills 1975, Forest et al. 1978). Indeed, Mills commented that Conesus Lake cyanobacteria were one of the most diverse assemblages of any lake (cited in Forest et. al, 1978). Colony-forming species of the genera *Dolichospermum, Aphanizomenon, Aphanocaspa, Oscillatoria, Lyngbia and Microcystis* are notable in abundance. According t*o* Makarewicz and Lewis (2014) there are two species of *Microcystis* in Conesus Lake*, M.aeruginosa and M. viridis*, and both are capable of producing toxic microcystins (Watanabe et al., 2014). Forest and colleagues state that *Anabaena* (now *Dolichospermum)* is "unquestionably common" and describe *M. aeruginosa* as a characteristic species in Conesus Lake, but never dominant as in other lakes. Mills (1975), however, reported a bloom in which *M. aeruginosa* comprised 13.1% of the total phytoplankton cell number. Only the diatom *Melosaira granulata* (26.5%) and the

cyanobacterium *Aphanizomenon flos-aquae* (19.6%) surpassed *Microcystis* in abundance. A 2014 study of phytoplankton by Makarewicz and Lewis was consistent with the observations of Forest *et al.* (1978) in reporting very large average May-September biovolumes of *Pseudoanabaena* (10%), *Anabaena* (6.7%) and *Oscillatoria* (4.5%), whereas the biovolume of the two *Microcystis* species were reported to be less than 0.6%.

It may be that some of the discrepancies between previous studies are due to differences in the timing of sample collection. Bosch and colleagues (2015, 2017, personal observations) have found that *Dolichospermum* species are prevalent in mid-summer blooms that typically start in late June- early July, whereas *Microcystis* tend to be more abundant in September and October blooms (Makarewicz *et al*, 2009b). Moreover, the density, timing and duration of the mid-summer blooms have been quite variable. In some years, *Dolichospermum*-dominated blooms have covered large sections of the north basin. In other years the blooms have been sparse and short lived, or they have persisted well into September (IB personal observations).

Because midsummer cyanobacterial blooms have the greater potential to impact summer recreational use of the lake, it is important to understand the timing and causes of these events. Our hypothesis is that wind-driven mixing of the hypolimnion initiate midsummer blooms by moving internally loaded phosphorus to surface waters. Initial efforts to examine this connection were hampered by a lack of real time data on lake temperature stratification and mixing. In 2016 and 2017, temperature array systems designed by one of us (KH) were deployed in the three basins of Conesus Lake. With these arrays in place we now have the capacity to observe water column mixing events in real time and to follow quickly with measurements of physicochemical and biological responses.

The results of the present study provide robust evidence of a link between wind-driven mixing on June 28 and a single-cell cyanobacterial bloom that peaked during July 4-11th. Moreover we provide evidence that a bloom of colonial cyanobacteria that peaked in August 11-15 was preceded by a major wind disturbance on July 30th and August 1st that increased P levels in surface waters. A particularly dense bloom recorded in early September followed major wind disturbances on August 28 and September 1.

III. METHODS

Sample collections under the auspices of the monitoring plan were made from June 13 to August 23rd in the central and south basins, which are the key regions of internal P loading in Conesus Lake (Bosch and colleagues, 2015, 2017). Collections were continued well into

September and array *in situ* temperature data are reported up to the October 24 turnover in the south basin. Hydrolab profiles and water samples were collected weekly or more frequently for analysis during the funded study period.

Lake stratification was monitored using temperature arrays deployed in each basin. One of the arrays (initially deployed in 2016) was placed in the northern basin at a depth of 10.8 m (Lat 42.812016 N -77.7124023 W). A second was placed in the south basin in 2017 and anchored at a depth of 17.9 m (Lat: 42.7643700 N Long: W77.7138824 W). The central basin array deployed in 2017 is anchored at 14.2 m (Lat: 42.793056 N Long: W77.7178761 W). In each array, sensors are positioned at approximately every meter from a depth of 4 m to the bottom of the water column. The sensors transmit temperatures every 15 min and these data are archived in a server located on the SUNY Geneseo campus (http://iotdb.geneseo.edu/streams/).

The Schmidt Stability indeces of the water column for each basin were calculated from array temperature data using R Statistical software and specifically a LakeAnalyzr package (Winslow and colleagues (*//cran.r-project.org/web/packages/rLakeAnalyzer/index.html*) that includes procedures for calculations of water column parameters. The Schmidt Stability Index is an estimate of the amount of energy (J/m^2) necessary to bring a lake to a uniform density. We also calculated the Relative Thermal Resistance to Mixing (RTRM), which is a measure of the energy required to mix water of two different temperatures and thus different densities ((http://www.ecosystemconsulting.com/pdfs/AAA%20RTRM.pdf). The RTRM value is a dimensionless number (Kortman, RW, Ecosystem Consulting Services).

Water column profiles were obtained with a Hydrolab 5a sonde equipped with sensors for depth (m) temperature (°C), photosynthetically active radiation (in $\mu Einsteins \cdot m^{-2} \cdot sec^{-1}$ of 400-700 nm wavelengths), chlorophyll equivalents (as millivolts, mV), conductivity ($\mu Siemens \cdot cm^{-2}$), dissolved oxygen ($mg \cdot L^{-1}$ and % saturation) and redox potential (mV). With the exception of the on board fluorometer, all sensors were calibrated within a few hours of sampling, in adherence to the procedures and recommendations of the manufacturer (OTT Hydromet).

Two independent measures of water transparency were recorded. Water turbidity as nephelometer turbidity units (NTU) was measured with a calibrated Hach 2100P turbidity meter meter. The Secchi depth was determined with a black and white 20-cm disk.

Samples for nutrient analyses were collected typically from the surface and every 3 m to within 1 m off the bottom using a Van Dorn water sampler. The water was stored in acid-washed plastic bottles and held in ice for transport. All sample containers were rinsed with the

water being collected prior to sample collection. In general, all procedures followed Standard Methods for the Analysis of Water and Wastewater (USEPA, 1999). Analyses of water samples for total phosphorus (TP; EPA method 365.1 Rev 2) were carried out at the NELAP and NYS accredited Life Sciences Laboratory in East Syracuse NY.

Seasonal patterns of cyanobacteria colony abundance were documented by counting freshly collected from the skim layer and from a depth of 0.3 m. Subsamples of 1 to 5 mL (depending on abundance) were initially taken from each collection and examined with a Wild stereomicroscope at 20X magnification. Counts of single cell cyanobacteria were carried out by placing subsamples of skim and grab collections in a hemocytometer and then counting cells using a fluorescence microscope under a FITC filter set.

Water samples for more detailed cyanobacterial species composition and distributional patterns were taken at depths of 0 (surface), 3, 6, 9, 12, 15, and 18 m in the southern basin and at 0, 3, 6, 9, and 12 m in the center basin. A Hydrolab DS5 was used to record *in vivo* phycocyanin from just below the surface of the water (0 m) to just above the sediment surface (~18 m in south and ~12 m in center basin). The water samples were transported to the water quality lab at SUNY-Brockport on ice. Three-hundred to five-hundred mL aliquots of each water sample were filtered through glass fiber filters and extracted with 90% alkaline acetone. Extracted samples were filtered using syringe filters (0.45-µm) and measured fluorometrically using standard methods (EPA Method 445.0). Cyanobacterial species abundance and composition were determined via the inverted microsope technique (Utermohl, 1958) using water samples preserved in 1% Lugol's solution. Biovolume for each species was calculated using cell counts (10-50 fields per magnification from 100x to 400x) and estimates of cell volume based on cell dimensions (400X) were obtained using a Wild Inverted microscope (Chislock et al., 2014; Makarewicz and Lewis, 2014).

IV. RESULTS AND DISCUSSION

Oxygen Depletion and Internal Loading of Phosphorus in the Hypolymnion

Temperature-mediated density stratification of the water column creates a physical barrier that minimizes exchange between the upper oxygenated regions of the lake (the epilimnion) and the colder dark depths (hypolimnion). In the hypolimnion, microbes respire much of the oxygen and release carbon dioxide. The hypolimnion thus becomes hypoxic or even anoxic (low or depleted of oxygen) and slightly acidic due to carbon dioxide buildup. Under

these conditions the hypolimnion and the sediment-water interface change from oxidizing to reducing, a process that is easily measured using oxidation-reduction sensors. Reducing conditions (~ <200 mv) tend to solubilize legacy phosphorus from the sediments into pore water and then by diffusion into the hypolimnion.

Trends in our data reflect these processes very clearly. The lake basins become stratified in May, as illustrated by the differences in temperature with depth **(Fig. 1)**. Oxygen loss starts soon after stratification and by late June-early July in the south basin and mid-July in the central basin there is very little oxygen left below a depth of 10 m (**Fig. 2, 3; Appendix I** contains the full set of Hydrolab profile data). The oxidation-reduction potential (ORP) drops below 150 mv by July 11 in the south basin (18 m) and by July 25 in the central basin (12 m), while it remains above 400 mv in the oxygenated epilimnion. AT this time there is evidence of TP buildup below 12 m in the south basin (**Table 1**). Concentrations of TP that were typically 17-21 $\mu g \cdot L^{-1}$ near the bottom increased to 82 $\mu g \cdot L^{-1}$ by July 21 and to 230 $\mu g \cdot L^{-1}$ by August 23, when the last samples of the season were collected. In the center basin, TP peaked at 999120 $\mu g \cdot L^{-1}$ on August 1 and declined to 56 $\mu g \cdot L^{-1}$ by August 23 (**Table 2**). This decline may have been due to significant water column mixing that took place between the sampling dates.

In 2018, the concentration of total phosphorus (TP) in the hypolimnion increased over the summer period of stratification in the south and center basin **(Tables 1 and 2)**. Sampling for this study ended in August 23, but the trends from previous studies indicate that internal loading would have continued into September (Bosch et al., 2017) and most likely until the fall turnover in mid October. Consequently, the numbers reported in this study likely underestimate the total amount of legacy phosphorus released from the sediment.

To examine the phenomenon of internal P loading in Conesus Lake comprehensibly we evaluated phosphorus profile data from five previous studies by SUNY Brockport and SUNY Geneseo. The total hypolimnetic TP buildup, daily and areal release rates show a great deal of variability in these estimates (**Table 3).** For example, the total TP load in 2004 was only 2358 Kg and release rates were 18.4 $Kg \cdot day^{-1}$ whereas in 2009 the total TP was 8042 Kg 87.4 $Kg \cdot day^{-1}$. These differences undoubtedly reflect natural differences in loading, but another possible reason for the variability is that sampling in the various studies differed in terms of timing and total duration. The estimates in **Table 3** provide a general picture of internal P loading, but a more complete study is needed before we can fully evaluate the magnitude of this phenomenon. Nevertheless some important insights can be gleaned from a complete analysis of the existing data. As shown in **Figure 4**, it is obvious that P loading is consistently highest in the south

basin, where near-bottom TP concentrations can exceed 500 µg/L. In contrast, the north basin hypolimnion shows little TP buildup. The exception is a small and slightly deeper region of the north basin, where moderate TP buildup has been documented (Bosch *et al.*, 2015). The central basin TP buildup is moderate, with typical TP concentrations exceeding 200 $\mu g \cdot L^{-1}$. Another important trend is that TP accumulation begins in late June and early July and it may continue well into autumn. This means that by including May in an internal loading analysis and not September and early October we are surely underestimating the bulk of internal P loading taking place. According the CE-Qual-W2TMDL model simulation on which the Conesus Lake TMDL is based (E.P.A. Region 2/N.Y. State D.E.C. *draft* TMDL, 2019) the average anoxic P loading in Conesus Lake for 2007-2014 was 10, 641 $Kg \cdot yr^{-1}$. More targeted sampling in 2019 bring the empirical estimate more in line with the model predictions.

Temperature, Stability and Full Mixing of the Water Column

Temperature data gathered from the *in situ* arrays in the three basins are shown in **Figure 1.** Green arrows along the x-axis highlight periods of significant mixing and longer black arrows point to the fall turnover. We identified at least ten events in which the north basin was mixed to at least a depth of 10 m. This frequent breakdown in stratification is consistent with data showing that the hypolimnion in the north basin remains partly oxygenated during most of the summer. Consequently internal P loading in this basin is negligible except in a small region of deeper water ("trough") near the eastern shore (Bosch and colleagues, 2015, also see **Fig. 4).** Complete mixing did not take place in the central or south basins until October, but the profiles show evidence of temperature disturbances that affect the hypolimnion to a depth of at least 12.2 m in the central basin and to 12.8 m in the south basin.

Calculations of water column resistance to mixing are consistent with the observation of greater stability in the south basin, which is likely due to its greater depth and volume. For example, on July 11 the Schmidt Stability Index of the south basin was nearly 4x higher than that of the north basin, and 3x higher than that of the central basin (**Fig. 5**). We also calculated the Relative Thermal Resistance to Mixing (RTRM) of the three basins over several weeks. The trends of RTRM (**Table 4 and Fig. 6)** are consistent with that of the Schmidt Index. The south basin has the highest total RTRM, while the north basin has the lowest and the central basin is typically intermediate in RTRM.

Table 5 lists some of the dates in which major mixing events occurred as shown by array temperature data in all three basins (see **Fig. 1**). Disturbances to stratification were consistently

associated with periods ranging from an hour to several days in which wind speeds exceeded 10 mph and wind gusts, in some cases, exceeded 25 mph. Major wind-related mixing events occurred throughout the summer, some having obvious effects on water column stability (e.g. Aug. 21, Sept 21-24). Events on June 28, July 31 and Aug 28-September 1 are linked to biological responses described in later sections of this report. The two later events were powerful enough to have increased oxygen saturation and ORP in hypolimnetic waters of the south and central basins, as shown in **Figures 2 and 3**.

Biological Responses

Data for indicators of phytoplankton biomass including turbidity, Secchi depth and chlorophyll *a* concentrations are reported in **Table 6** for the south basin and **in Table 7** for the central basin. The average and standard deviation of chlorophyll *a* in the upper 6 m of the water column was 7.8±3.3 $\mu g \cdot L^{-1}$ for the south basin and 7.7±2.1 $\mu g \cdot L^{-1}$ for the central basin. These are very typical averages for Conesus Lake. The average summer Secchi depth was also close to typical with 2.2 m for both basins. Lastly, the TP average for the south basin was 17 $\mu g \cdot L^{-1}$. This was lower than the 21.9±1.7 $\mu g \cdot L^{-1}$ reported by Makarewicz and Lewis in 2014. Low sample size for the center basin did not permit a valid calculation of an average TP. The Carlson's Trophic State Index calculated for chlorophyll *a* (TSI=50.8), Secchi depth (TSI=48.6) and TP (TSI= 45.0) in the south basin resulted in an average TSI of 48.6, which is slightly lower than the long term average of 49.3 reported by Makarewicz and Lewis in 2014 and nearly identical to values reported since 2004. The indication is that the trophic state of Conesus Lake remains remarkably stable.

According to the indicators of phytoplankton biomass and to microscope counts of cyanobacterial numbers, the lake experienced several blooms over the growing season. The first was detected on June 28 with chlorophyll *a* values in the epilimnion of the south basin increasing from 7.1 $\mu g \cdot L^{-1}$ on June 21 to 11.4 $\mu g \cdot L^{-1}$ (**Table 6**). Microscope analyses showed that this was a relatively moderate bloom of less than 4 colonies $\cdot mL^{-1}$ dominated by *Dolichospermum, Oscillatoria* and *Gomphosphaeria spp.* (**Table 8**). By July 4 the characteristics of the bloom had changed. Fewer colonies were observed but it was obvious from the chalky green color of the lake that a different type of bloom was in progress. Water samples taken from about 0.3 m below the surface were examined under 400x magnification using a fluorescence microscope. The dominant phytoplankters in these samples were single-celled cyanobacteria at concentrations of about 250 x 10^3 cells $\cdot mL^{-1}$ (**Table 9).** Other indicators of phytoplankton biomass were consistent

with this observation, including chlorophyll *a* values that surpassed 10 $\mu g \cdot L^{-1}$, a very shallow Secchi depth of 0.9 m and high water turbidity of 8.7 NTU (**Tables 6, 7**). Bloom conditions persisted for more than a week but by the 16th of July the number of cells had declined to near background levels (~35 x 10^3 mL^{-1}). Blooms of single-celled cyanobacteria have previously been documented for Conesus Lake (Bosch and colleagues, 2015). The dominant single- celled cyanobacteria in 2015 were assigned to the genera *Synechococcus* and *Synechocystis,* which have been reported as abundant in Conesus Lake by earlier workers (Forest et. al., 1978). We believe that the single cell blooms in 2018 were dominated by the same species.

After the early July bloom of single-celled cyanobacteria a relatively clear-water period ensued, as shown by the low average chlorophyll a concentration of 6.56 $\mu g \cdot L^{-1}$, average turbidity of 2.19 NTU, a Secchi depth of 2.4 m (**Tables 6 &7**), cyanobacteria colony counts of 0.2-0.5 mL^{-1} and single cell cyanobacteria counts of 32-36 x10^3 mL^{-1}. Sustained winds of 10-12 mph gusting to 16 mph out of the NNW on July 30 may have brought about a change in conditions. There is evidence of temperature warming to depths of 12 m all along the lake, and Hydrolab profiles on July 30 and Aug. 1 showed increases in oxygen saturation and redox potential to a depth of 12 m. Analysis of water samples by Dr. Michael Chislock of SUNY Brockport indicated that soluble reactive phosphorus and TP concentrations increased by 39% and 25% and ammonia concentrations changed from not detectable to 5.3 $\mu g \cdot L^{-1}$. By August 11, cyanobacterial colonies in the south and central basins had increased to 4.1 mL^{-1} and 3.1 mL^{-1} and to 7.2 and 4.3 mL^{-1} by August 15 (**Table 8**). The dominant groups in this bloom were species of *Dolichospermum*, *Microcystis* and *Woronichinia*.

As evident in **Figure 1** and shown in **Table 5,** the next major wind events in the area occurred on August 21, 29 and Sept 1. All of these events caused major disruptions of stratification, increasing oxygen content and ORP at least to a depth of 12 m (**Fig. 2 and 3)**. By September 1, average chlorophyll *a* values in the epilimnion had increased by 50% to > 12 $\mu g\ L^{-1}$ and cyanobacterial colonies were abundant in surface waters. Average chlorophyll *a* concentrations remained high (12.5 $\mu g \cdot L^{-1}$) and high colony numbers persisted until at least the last sample collection of the season on September 13. Collections of phytoplankton from different depths were made on that day and in the next section we provide an analysis of the composition and biovolume of cyanobacteria species in the community.

Cyanobacteria Species Composition and Distribution

Chlorophyll *a* provides a coarse estimate of phytoplankton biomass in lakes. In general, chlorophyll *a* peaked in the upper portion of the epilimnion (0 to 6 m) (**Fig. 7**) on most dates. Epilimnetic chlorophyll *a* concentrations ranged from 4.80 to 19.61 $\mu g\ L^{-1}$, with an average of 7.76 $\mu g \cdot L^{-1}$. In addition to variation across depths, there was also considerable variation from month-to-month. Some of this monthly variability in chlorophyll can be attributed to several wind-driven mixing events as well as seasonal shifts in phytoplankton composition.

Given that cyanobacteria are the primary taxa responsible for freshwater harmful algal blooms, there is considerable interest in methods to rapidly assess the abundance of these taxa. Phycocyanin is a pigment produced by cyanobacteria, and *in vivo* measurements of this pigment are often used to provide practical, real-time estimates of potential cyanobacterial hazards in lake monitoring. Our *in vivo* phycocyanin data indicated that cyanobacteria abundance, similar to chlorophyll *a*, peaked in the epilimnion (0-6 m) (**Fig. 8**). In addition to variation in phycocyanin across depths, we also observed considerable temporal variation. Based on observed maximum phycocyanin levels on 28 June and 13 September 2018 (**Fig. 8**), these were the two dates selected for microscopic identification and enumeration of cyanobacteria.

We observed considerable seasonal shifts in the size structure of cyanobacterial assemblages in Conesus Lake. *Dolichospermum* species were observed following wind-driven mixing on 28 June (**Table 10**). However, overall biovolume for cyanobacterial species was relatively low on this date, with biovolume being consistent across epilimnion depths (0-6 m) (**Fig. 9**). Subsequently, a single-celled cyanobacterial bloom occurred in early July, which peaked during 4 to 11 July. Most importantly, we observed the development of a HAB event in mid-September, with *Dolichospermum*, *Microcystis*, and *Woronichinia* sp. being the dominant taxa (**Table 11**). Cyanobacterial filaments and colonies were densest near the surface, with peak biovolumes at 0 and 3 m. Overall cyanobacterial biovolume was over two orders of magnitude higher on 13 September than 28 June (**Fig. 9**).

V. CONCLUSIONS

Summer 2018 averages for indicators of water quality including total phosphorus, chlorophyll *a* and Secchi depth were comparable to those reported in recent years by Makarewicz et al. (2009, 2014). A Trophic State Index of 48.6 continues to place Conesus Lake within the range of a typical meso-eutrophic lake.

Anoxic internal loading of phosphorus in the hypolimnion during the period of stratification was relatively low compared to previous years. There is some uncertainty in this and previous estimates because researchers have sampled at different times and for different durations. All of the studies are consistent in showing that release of phosphorus from the sediments begins in late June and likely continues until fall turnover in the south basin, which in 2018 occurred in October. The south basin, due to its larger volume and greater depth, contributes the bulk of internally loaded phosphorus, followed by the central basin and the very shallow north basin. A more detailed study of internal loading is recommended. Sampling for any future study should measure TP and SRP in the three basins and collect samples from mid June into October. Such a detailed study would provide a rigorous baseline that could be used to evaluate any efforts to reduce internal P loading in Conesus Lake.

Strong winds during the summer caused considerable mixing of the lake water column below the thermocline, at times as deep as 12 m. This mixing delivered phosphorus to surface waters during periods when P supplies were very low and limiting to phytoplankton growth. We obtained robust evidence linking wind-driven mixing events on June 28, July 31 and August 28-Sept. 1 to succeeding cyanobacterial blooms. Cyanobacterial biovolume was over two orders of magnitude higher on 13 September than 28 June. This is consistent with the high volume of mixing and delivery of phosphorus to surface waters that was occurring by this time of year. Peak biomass occurred near the surface and primarily from 0-6 m in the epilimnion. The dominant species as in previous years were *Dolichospermum*, *Microcystis*, and *Woronichinia* sp.

The increasingly apparent role of internally loaded phosphorus as a proximate cause of recurrent summer cyanobacterial blooms in Conesus Lake suggests that any measures designed to reduce internal loading of P should be effective in minimizing the risk of summertime HABs. Aeration or oxygenation of the hypolimnion while avoiding disruption of the thermocline is an environmentally sound strategy that has been used successfully for P abatement in many lakes and reservoirs. This approach, although costly, may be preferable to use of chemicals such as alum that pose some degree of risk to the health of this valuable ecosystem.

Acknowledgements

Funding for this work was provided by a grant from the Livingston County Planning Department. The authors would like to acknowledge the support given to our research program and to our student researchers by Anne Baldwin, Director of Sponsored Research SUNY Geneseo, and Betsy Colon, Contracts and Grants Associate SUNY Geneseo, and Laura Merkl at Contracts and Grants Administrator for the Research Foundation at SUNY Brockport.

VI. REFERENCES

Arar, E.J., and G.B. Collins. Method 445.0 in vitro determination of chlorophyll a and pheophytin in marine and freshwater algae by fluorescence. U.S. Environmental Protection Agency, Washington, DC, 1997.

Bosch, I, J.C. Makarewicz, J.P. Emblidge, D.A. Johnson and M.D. Valentino. 2001. Population Studies of Eurasian watermilfoil and Zebra Mussels in Conesus lake, NY (Summer 2000). Report to the Livingston County Planning Department. 37 pp

Bosch, I., T. Shuskey, T. Collins and A. Smith. 2013. Studies of Adult and Larval Zebra Mussel Populations in Conesus Lake, NY (Summer 2013). Report to the Livingston County Planning Department. 32 pp

Bosch I, D. Connors, C. McCabe, G. Wong, A. Bowling and A. Kubik. 2015. Linkage Between Water Column Mixing of Phosphorus and Onset of Cyanobacterial Blooms in Conesus Lake, NY. Report to the Livingston County Planning Department. 63 pp

Bosch, I. E. Reiter, M. Roncone, K. Rounds, K. Warner, S. Guyton, S. Bosch and K. Hanafin. 2017. Monitoring of Water Quality, Water Column Mixing and Blooms of cyanobacteria in Conesus Lake (NY), Summer 2017.

Chislock, M.F., K.L. Sharp, and A.E. Wilson. 2014. *Cylindrospermopsis raciborskii* dominates under very low and high nitrogen-to-phosphorus ratios. *Water Research* 49: 207-214.

Forest, H.S., Wade, J.Q., and Maxwell, T.F. 1978. The Limnology of Conesus Lake. *In Lakes of New York State: Ecology of the Finger Lakes*, ed. J.A Bloomfield, pp. 122-225. New York: Academic Press

Makarewicz, JC., I.Bosch and T.Lewis. 2004. Conesus Lake Limnology: Including Lake Chemistry, Phytoplankton and Estimates of Internal Loading in 2004. Report submitted to the Livingston County Planning Department. 13 pp. Available at *Technical Reports*. Paper 33. http://digitalcommons.brockport.edu/tech_rep/33.

Makarewicz, J.C. and Theodore W. Lewis. 2009. Conesus Lake Limnology 2009: Water Quality of USDA Monitored Watersheds, Internal Hypolimnetic Phosphorus Loading, Lake Chemistry, and Status of the Zooplankton. Report to the Livingston County Planning Department. 67 pp. Available at *Technical Reports*. 9. http://digitalcommons.brockport.edu/tech_rep/9

Makarewicz, J.C. *et al*. 2009b. Spatial and Temporal Distribution of the Cyanotoxin Microcystin-LR in the Lake Ontario Ecosystem: Coastal Embayments, Rivers, Nearshore and Offshore, and Upland Lakes. *Journal of Great Lakes Research*, 35:83-89

Makarewicz, J.C. and Theodore W. Lewis. 2014. Trophic Status of Conesus Lake 2014: Long-Term Trends in Lake Chemistry and the Plankton Community. Report to the Livingston

County Planning Department. 69 pp. Available at *Technical Reports*. 130. http://digitalcommons.brockport.edu/tech_rep/130

Mills, E.L. 1975. Thesis (Ph.D.) Cornell Univ., Jun 1975. Phytoplankton composition and comparative limnology of four Finger Lakes, with emphasis on lake typology.

Raikow, D.F. 2004. Dominance of the Noxious Cyanobacterium *Microcystis aeruginosa* in Low-Nutrient Lakes is Associated With Exotic Zebra Mussels. *Limnology and Oceanography* # 49 pp 482-487

Tang, Huijuan. H. Vanderploeg, T.H. Johengen and J.R. Liebig and. 2014. Quagga mussel (*Dreissena rostriformis bugensis*) selective feeding on phytoplankton in Saginaw Bay. *J. Great Lakes Research* 40: 83-94.

USEPA. 1979. *Methods for the Chemical Analysis of Water and Wastes*. Environmental Monitoring and Support Laboratory. Environmental Protection Agency. Cincinnati, Ohio. EPA-600/4-79-020

Vanderploeg H.A. *et al.*, 2001. Zebra mussel (*Dreissena polymorpha*) selective filtration promoted toxic *Microcystis* blooms ub Saginaw Bay (Lake Huron) and Lake Erie. *Can. J. Fish. Aquat. Sci.* 58: 1208-1221.

Watanabe, M.F., K Harada, K Matsuura, H. Kawal and M. Suzuki. 1988. Toxins contained in *Microcystis* species of cyanobacteria (blue-green algae). *Toxicon* 26: 1017-1025

VII. TABLES AND FIGURES

Table 1. Total phosphorus in the central basin of Conesus Lake during the growing season in 2018. Samples were collected over a depth of 18-19 m near the long term monitoring station established by the N.Y. State D.E.C.

Total P (µg/L)	6/13	6/21	7/6	7/21	8/23
Surface	19				20
3 m	18	24	16	8.5	19
6 m	14	17	18	11	22
9 m	15	15	16	5.3	25
12 m	18	11	12	28	20
15 m	12	12		12	130
18m	17	21	19	82	230

Table 2. Total phosphorus in the center basin almost directly offshore of the Geneseo water plant over 12-14m of water.

Total P (µg/L)	6/13	6/21	7/6	8/1	8/23
Surface		24	16	7	22
3m			20		22
6m			15		22
9m	23		13	25	18
12 m Bottom	27	23	14	120	56

Table 3. Whole lake Internal hypolimnetic P loading estimates for Conesus Lake from studies by Makarewicz and colleagues 2004, 2009, 2012 and Bosch and Colleagues 2017-2018. All TP analyses were carried out by ELAP certified laboratories at SUNY Brockport and at the Life Sciences Laboratory, Inc.

Year	Dates	Days Start-End	Kg of TP Loaded	% of All Lake TP	Kg P /day Loaded	g P/m^2/d
2004	5/1- 9/14	128	2358	45.0	18.4	1.84
2009	5/19- 8/18	92	8041	74.3	87.4	8.74
2012	5/22- 8/14	84	6240	68.9	61.2	6.12
2017	6/12- 9/12	92	5797	67.2	54.8	5.48
2018	6/13- 8/13	61	2760	51.5	38.9	3.89
-	-	**Mean**	**5039**	**61.4**	**52.2**	**5.21**
-	-	**St. Dev.**	**2164**	**11.2**	**25.7**	**2.57**

Table 4. The total relative thermal resistance to mixing (RTRM) calculated for each of the basins in Conesus Lake over the 2018 sampling season. These values of resistance to mixing are consistent with the Schmidt Index in showing the south basin to be the most stable, followed by the central basin and the north. Temperature data was obtained from the in situ temperature arrays.

Date	Total RTRM North	Total RTRM Central	Total RTRM South
13-Jun	117.2	165.1	216.7
21-Jun	151.8	239.4	257.8
11-Jul	299.6	335.2	360.7
30-Jul	247.1	283.6	320.3
15-Aug	253.3	303.6	360.7
23-Aug	222.3	262.9	278.5

Table 5. Weather conditions associated with significant water column mixing (M) from first stratification to fall turnover in 2018 (T). Temperature data collected with *in situ* arrays and days of significant mixing are shown in **Figure 1**. Weather data were from the Dansville Municipal airport are archived by the Weather Underground.

Date	North Basin	Central Basin	South Basin	Wind Conditions (Dansville Municipal Airport)
June 5	M	No data	-	2-12PM: 9-14 mph sustained ENE, SSW; rain 0.05 in
June 12	M	No data	M	1-3PM gusts 15 mph, 9AM-3PM sustained 12 mph NNW
June 28	M	M	M	2-4 PM sustained **10-12** mph SSE; 0.08in
July 22	M	M	M	3-6 PM gusts 28 mph**,** 12-7PM sustained 10-21 mph SSW**;** 1.16in
July 31	M	M	M	1-2 PM Gusts to **16** mph, 1-6PM sustained 10-12 mph NNW
Aug. 21	M	M	M	2 hr gusts to 20 mph, 10AM- 6PM sustained 10-14 mph; 0.25in
Aug 29	M	M	M	6 hr gusts 17-31 mph, NNE to S; 0.69 in during 4-5 PM T-storm;
Sept. 1	M	M	M	9-11AM gusts 13-20 mph, 10AM-noon sustained 10-12 N; 0.21in
Sept 21	M	M	M	8 AM-6 PM gusts 28mph, sustained 10-16 mph; 0.3in
Sept 24	T	M	M	4 hr gusts 22mph, 10AM-Mid sustained 10-14mph NNW; 0.05in
Oct 17	-	T	M	2-10 PM gusts 20-24mph/sustained 10-14mph E, SE; 0.18in
Oct 24		-	T	7-9AM gusts 20mph, 6 AM-5PM sustained 10-14mph SE

Table 6. Turbidity, acetone extracted chlorophyll *a* concentrations and Secchi depth for the Southern Basin Station from June 13 to Sept. 27, 2018

Date	Depth (m)	Turbidity (NTU)	Chl α (µg/L)	Secchi Depth (m)
6/13/18	0		4.8	3.6
	3		4.7	
	6		5.2	
	9		5.0	
6/21/18	0		4.8	2.8
	3		9.7	
	6		7.8	
	9		5.9	
6/28/18	0		13.1	2.5
	3		14.0	
	6		10.3	
	9		8.4	
7/11/18	0	*6.5	7.5	*1.2
* single cell bloom	3		8.9	
	6		7.3	
	9		4.8	
7/16/18	0	1.9	4.6	1.9
	3		6.3	
	6		6.3	
	9		3.9	
7/21/18	0	2.1	5.6	2.1
	3	2.1	5.7	
	6	1.5	5.8	
	9	1.5	5.1	
	12		3.5	
7/24/18	0	1.44	4.7	2.5
	3	1.85	8.0	
	6	1.96	7.9	
	9		6.3	
7/27/18	0	1.84	6.6	2.3
	3	1.83	7.4	
	6	1.54	7.6	
	9	2.60	5.8	

	Table 6	continued		
Date	**Depth**	**Turbidity**	**Chl α**	**Secchi**
7/30/18	0	1.82	4.7	2.5
	3	1.46	5.4	
	6	1.74	4.1	
	9	2.21	5.8	
	12	2.32	6.2	
8/1/18	0	1.56	2.9	2.0
	3	1.28	5.7	
	6	1.45	5.8	
	9	2.91	9.8	
	12	2.07	5.5	
8/10/18	0	1.22	6.17	2.3
	3	1.29	6.74	
	6	1.63	13.32	
	9	2.15	9.74	
8/15/18	0	2.05	6.4	2.9
Cyano	3	1.69	8.9	
bloom	6	1.65	7.5	
	9	2.19	7.9	
8/23/18	0	2.25	7.38	2.4
* Cyano	3	2.65	8.04	
bloom	6	2.67	8.15	
	9	8.15	19.92	
9/1/18	0	3.22	12.01	1.5
	3	2.42	12.44	
	6	3.38	11.86	
	9	1.86	7.20	
9/13/18	0	5.89	19.61	1.2
	3	3.07	11.82	
	6	1.47	6.02	
	9	1.34	1.69	
9/27/18	0	5.98		1.5
	3	3.25		
	6	4.51		
	9	1.34		

Table 7. Turbidity, acetone extracted chlorophyll *a* and Secchi depth for the Central Basin.

Date	Depth (m)	Turbidity (NTU)	Chl α (µg/L)	Secchi Depth (m)
6/13/18	0	1.2		3.3
	3			
	6			
	9		3.63	
6/21/18	0	1.8	9.52	2.8
	3		10.31	
	6			
	9			
6/28/18	0	2.2	8.89	2.4
	3		10.93	
	6			
	9			
7/5/18	0	8.78	9.79	0.9
* Single	3	8.63	10.19	
bloom	6		10.02	
	9		5.09	
7/11/18	0	6.6	10.15	1.2
	3		10.58	
	6			
	9		5.85	
7/16/18	0	3.4	1.98	1.9
	3		7.64	
	6		6.49	
	9		1.17	
7/21/18	0	2.0		2.0
	3	1.94	6.95	
	6	1.86	6.69	
	9	1.60	6.11	
7/24/18	0	3.93		2.3
	3	1.59	9.08	
	6	1.65	8.64	
	9		6.99	
7/27/18	0	3.0	5.98	2.5
	3	1.8	6.49	
	6	1.95	6.85	
	9	5.34	8.75	
7/30/18	0	3.1	5.41	2.7
	3	1.47	6.18	
	6	1.62	6.91	
	9	2.9	5.45	
8/1/18	0	1.3	5.72	2.0
	3	1.53	5.8	
	6	1.73	5.84	
	9	1.52	5.53	
8/10/18	0	1.28	6.6	2.5
	3	1.69	6.71	
	6	1.45	8.77	
	9	2.19	9.23	

		Table 7 Continued		
Date	**Depth (m)**	**Turbidity (NTU)**	**Chl α (µg/L)**	**Secchi Depth (m)**
8/15/18	0	1.74		
	3	1.49	8.27	
	6	5.29	9.19	
	9	3.88	15.86	
8/23/18	0	2.2	10.97	
	3	4.14	9.02	
	6	2.24	8.26	
	9	1.81	4.88	
9/1/18	0	3.89	11.56	
	3	2.62	13.39	
	6	2.28	11.32	
	9		2.94	

Table 8. Counts of cyanobacteria colonies made at magnifications of 10-50x on a stereomicroscope. The numbers show a minor bloom occurred in late June, and another in early to mid August, as regular sampling for the summer was completed.

Collection Date	Skim Colonies per mL	0.3 m Colonies per mL	Comments on Species
South Basin			
28-Jun	0.8	3.6	*Dolichospermum* trichomes, *D. circinalis* large clumps; *Oscillatoria*, *Gom*
21-Jul	0.2	0.0	*Dolichospermum* trichomes, clumps
24-Jul	0.5	0.5	*Dolichospermum* trichomes small, coil; small *Microcystis, Oscillatoria*
11-Aug	4.4	3.8	*Dolichospermum* trichomes, few clumps; small *Microcystis,*
15-Aug	6.8	7.5	*Dolichospermum* coils, *Oscillatoria*
Center Basin	-	-	-
21-Jul	0.1	0	*Dolichospermum* trichomes
24-Jul	0.5	0.5	*Dolichospermum* coils, *Oscillatoria*
11-Aug	3.4	2.8	*Dolichospermum* trichomes, few clumps; small *Microcystis, Woronichinia*
15-Aug	4.4	4.2	*Dolichospermum* trichomes, helical and large clumps; *Woronichinia,* small *Microcystis*

Table 9. Counts of single celled cyanobacteria from the center and south basin, made using a fluorescent microscope. The numbers show a bloom occurred in early July, corresponding to a blue-green chalky color throughout the lake, high turbidity and reduced Secchi depth.

Date Collected	Collection Site	Depth (m)	10^3 Cells/ml	Turbidity 0-3 m (NTU)	Secchi Depth (m)
4-July	Long Point	0.3	250 ± 6	8.67	0.9
5- July	Center	3	261± 9	8.78	0.9
11-July	South	3	178 ± 4	6.50	1.2
16-July	South	0.3	57 ± 4	2.00	1.9
21-July	Center	0-6	33 ± 9	2.00	2.0
21-July	South	0-6	52 ± 5	2.10	2.1
24-July	Center	0-3	32 ± 2	1.63	2.3
24-July	South	0-3	36 ± 3	1.64	2.5

Table 10. Biovolume of Conesus Lake cyanobacteria across depths for 28 June 2018. No cyanobacteria were detected below 6 m deep. *ND = not detected

Taxon	Biovolume (0m) (μm^3 mL^{-1})	Biovolume (3m) (μm^3 mL^{-1})	Biovolume (6m) (μm^3 mL^{-1})
Aphanocapsa delicatissima	199	ND	ND
Dolichospermum circinale	1,318	5,933	ND
Dolichospermum spiroides	6,531	4,639	5,190
Gomphosphaeria lacustris	3,044	ND	ND
Merismopedia warmingiana	8	ND	ND
Total	11,100	10,572	5,190

Table 11. Biovolume of Conesus Lake cyanobacteria across depths for 13 September 2018. No cyanobacteria were detected below 6 m deep. *ND = not detected

Taxon	Biovolume (0m) (μm^3 mL^{-1})	Biovolume (3m) (μm^3 mL^{-1})	Biovolume (6m) (μm^3 mL^{-1})
Aphanocapsa delicatissima	3,470	ND	ND
Dolichospermum circinale	2,811,862	396,969	ND
Dolichospermum spiroides	714,144	550,111	34,112
Merismopedia warmingiana	940	ND	ND
Microcystis viridus	49,726	ND	27,552
Oscillatoria sp.	617	19,757	ND
Woronichinia sp.	2,579	4,742	ND
Total	3,583,338	971,579	61664

FIGURES

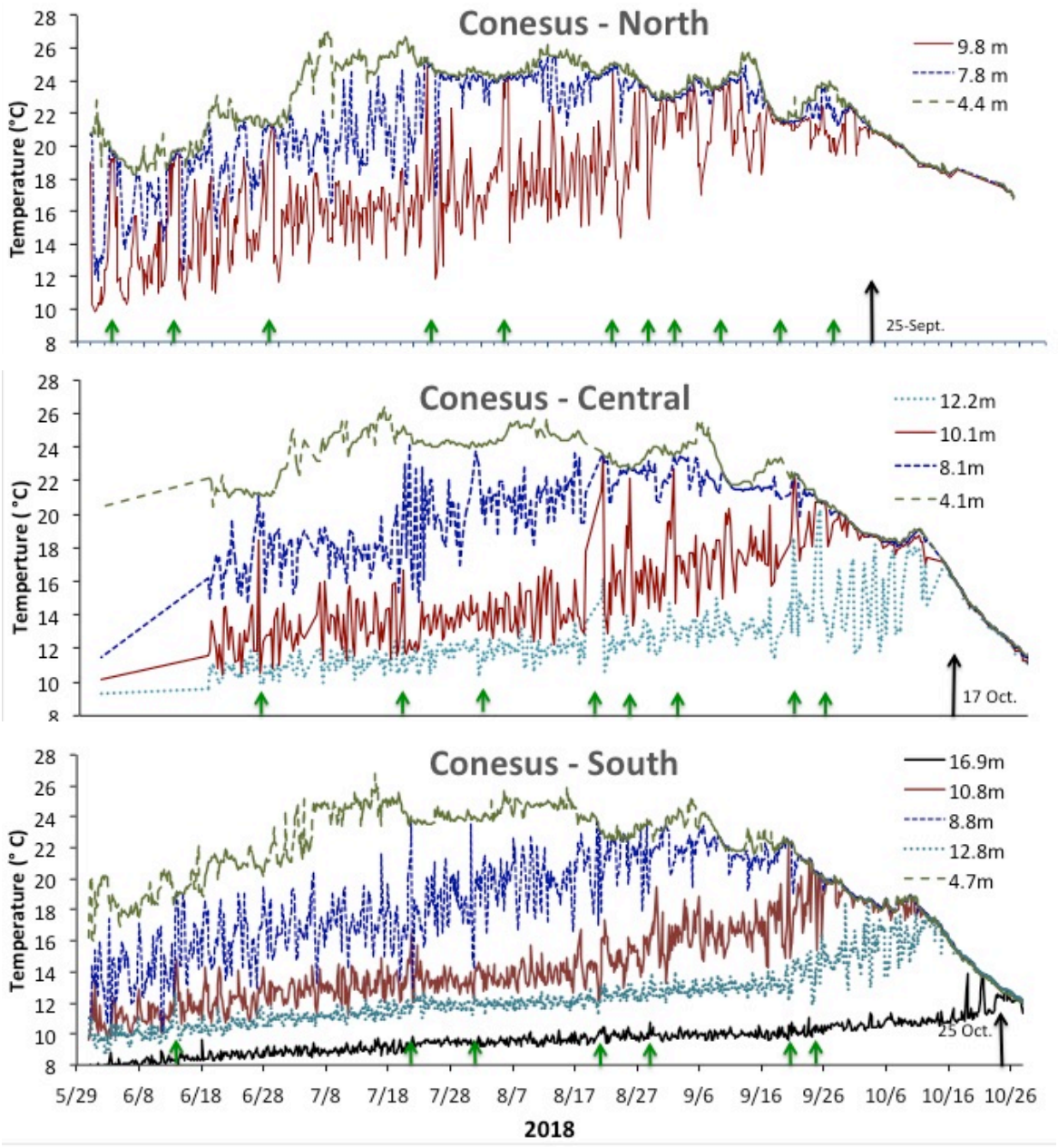

Figure 1. Data from *in situ* temperature arrays showing water column temperatures in Conesus Lake. The green arrows highlight the major mixing events, as indicated by warming of deeper waters. Longer black arrows point to the fall turnover.

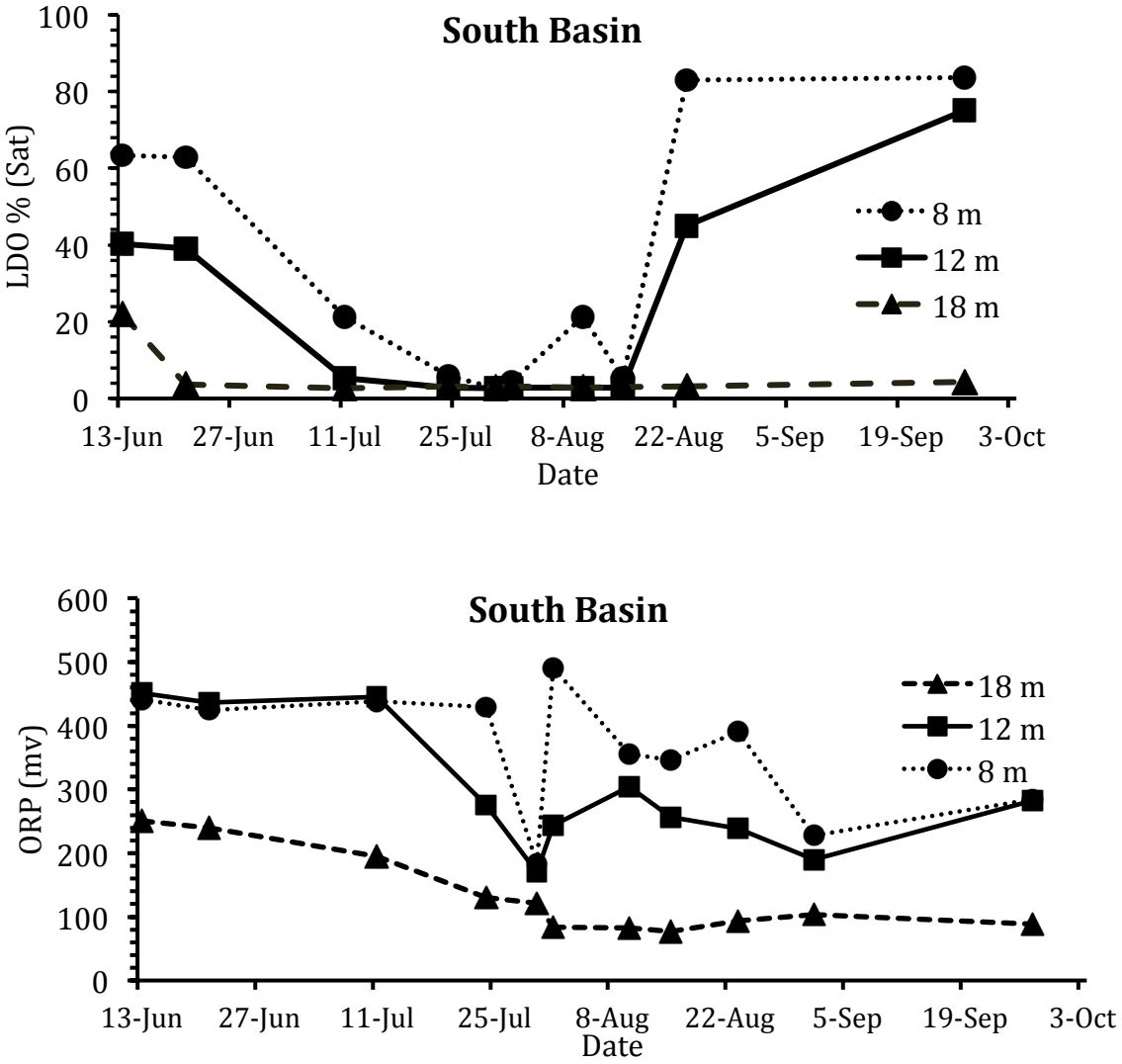

Figure 2. Oxygen saturation (top) and ORP (Oxidation-Reduction Potential) for the south basin in 2018.

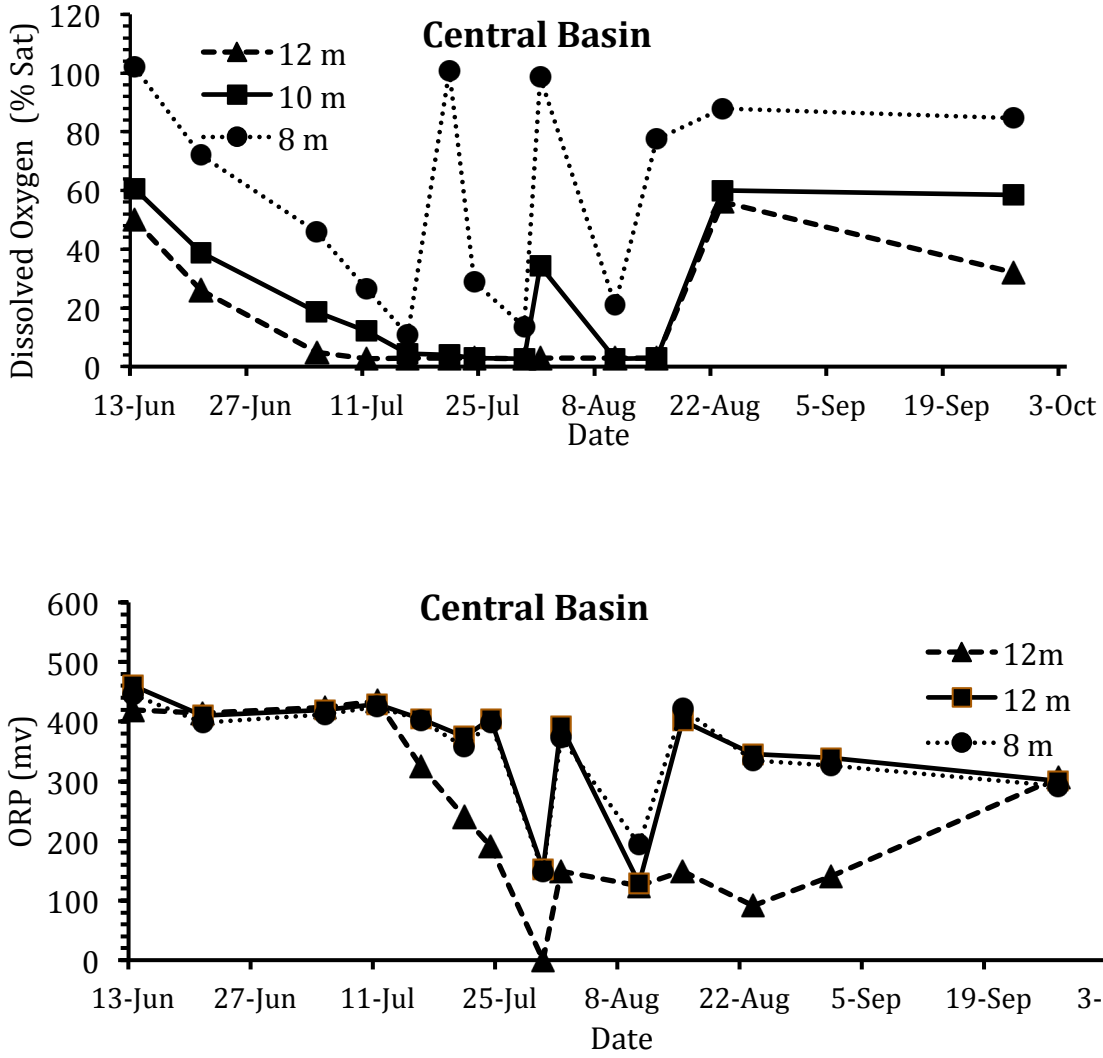

Figure 3. Oxygen saturation (top) and ORP (Oxidation-Reduction Potential) for the central basin in 2018.

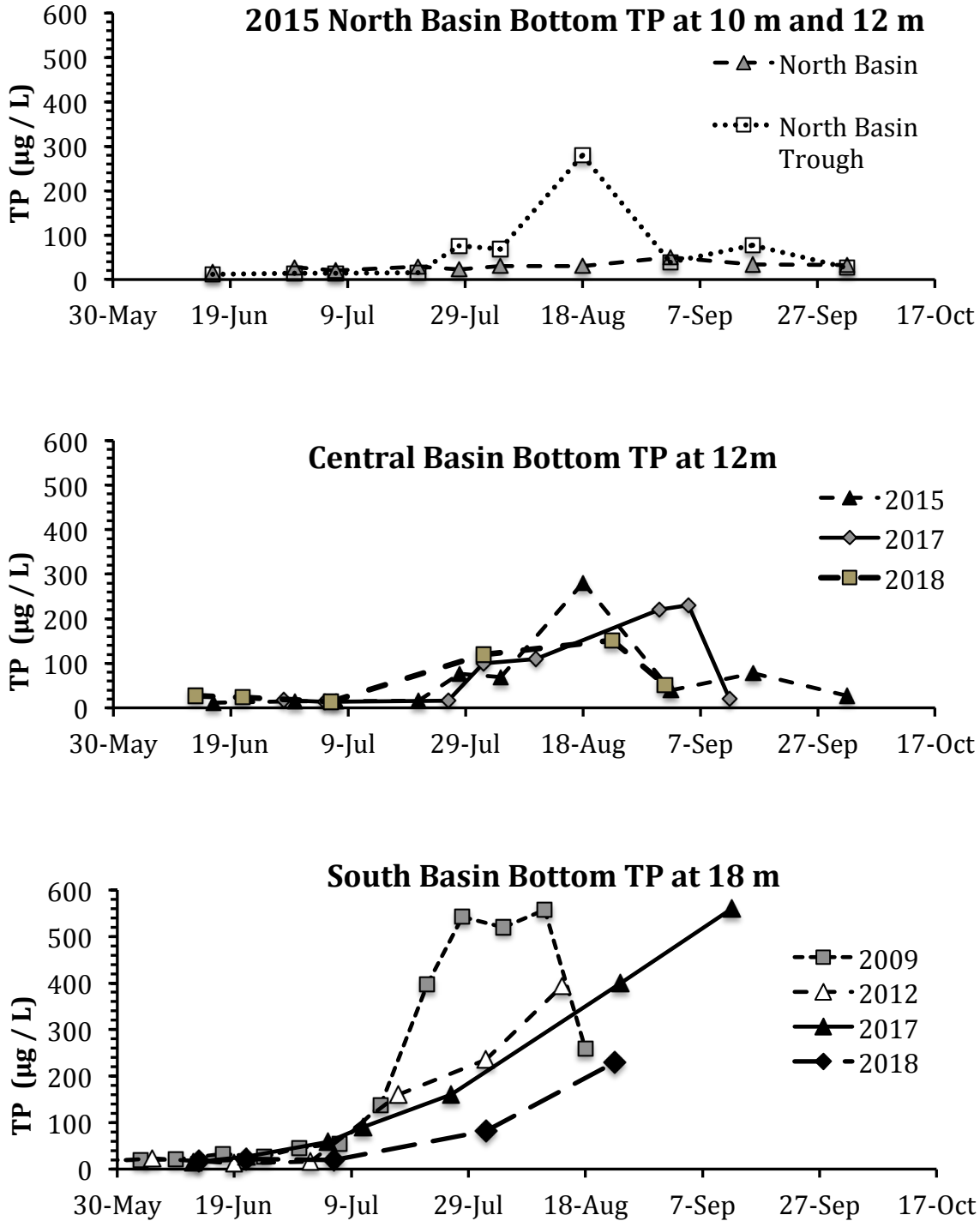

Figure 4. Build up of TP measured approximately 1m off the bottom in each of the three Conesus Lake basins. Very little TP accumulates in the North Basin (top), with the exception of a small area of deeper water ("north basin trough") near the east shore. Data are from studies by Makarewicz and colleagues (2009, 2012) and Bosch and colleagues (2015, 2017 and this study).

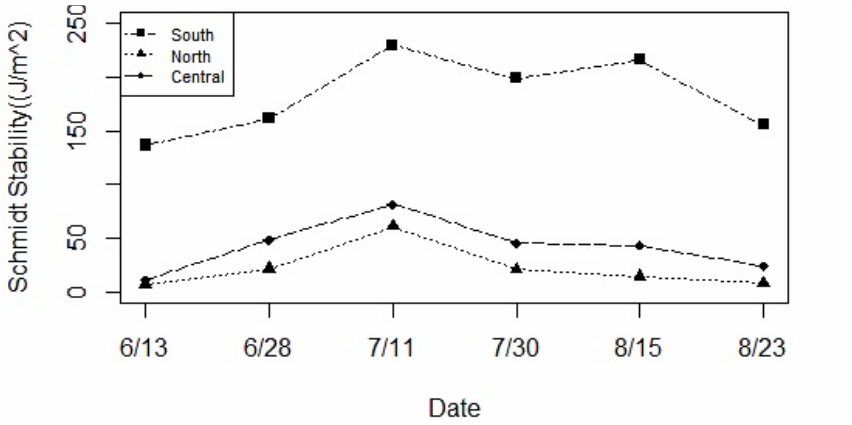

Figure 5. The Schmidt Stability Index for the three basins and showing the markedly greater stability of the south basin. It would take 4.5 times more energy to create a uniform water temperature in the south basin than in the north basin.

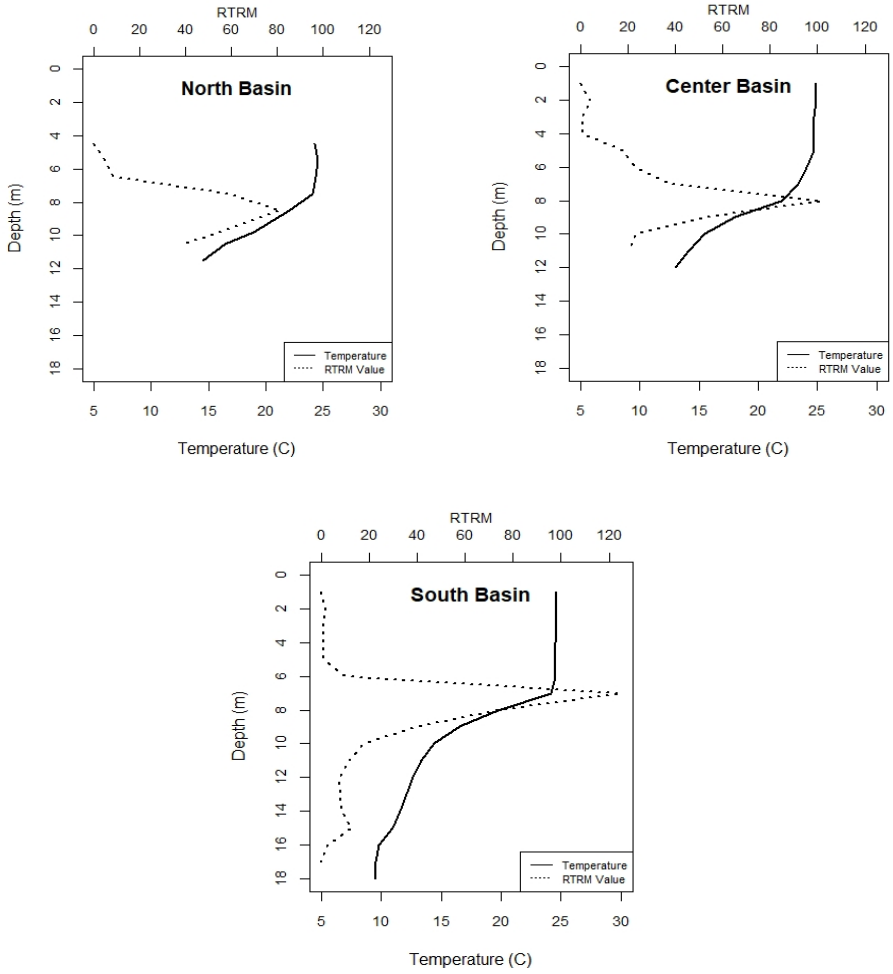

Figure 6. The Relative Thermal Resistance to Mixing is shown in these graphs for all three basins, as calculated from temperature profiles on July 30, 2018. The peak of each curve represents the maximum RTRM whereas the area between each curve and the y-axis represents the maximum RTRM.

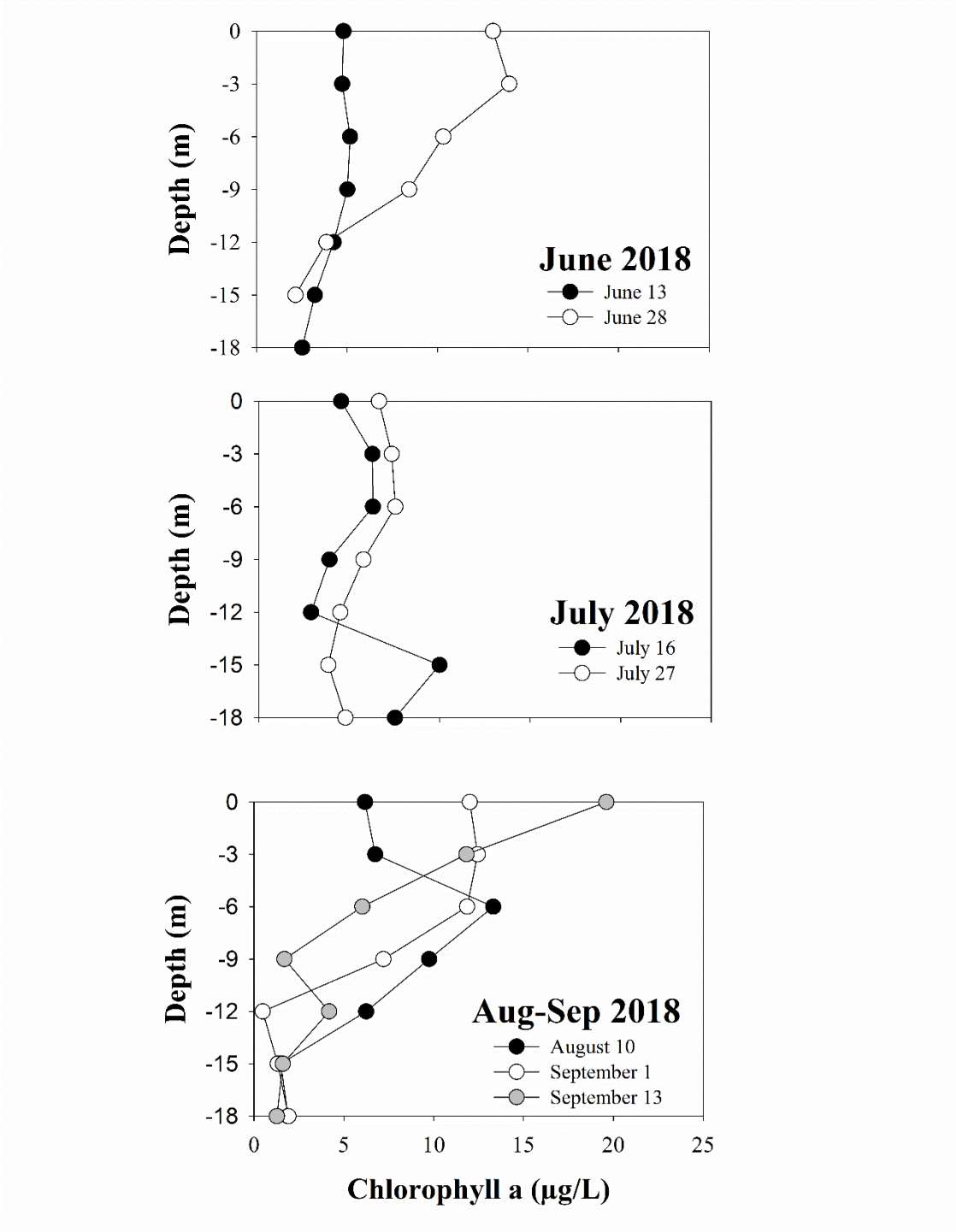

Figure 7. Depth profiles of phytoplankton biomass as chlorophyll *a* for selected dates in June, July, and August-September of 2018.

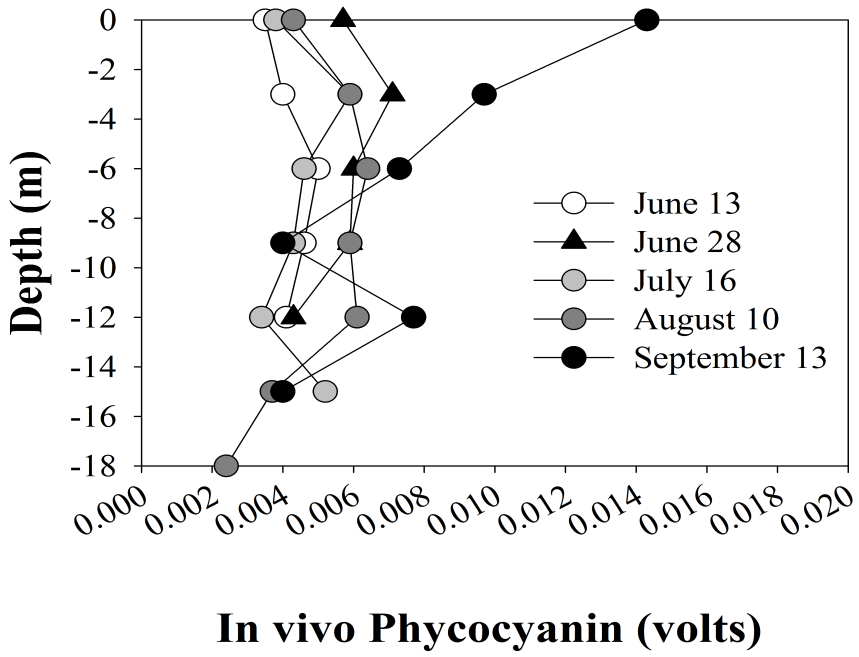

Figure 8. Depth profile of *in vivo* phycocyanin for selected dates in June, July, August, and September of 2018.

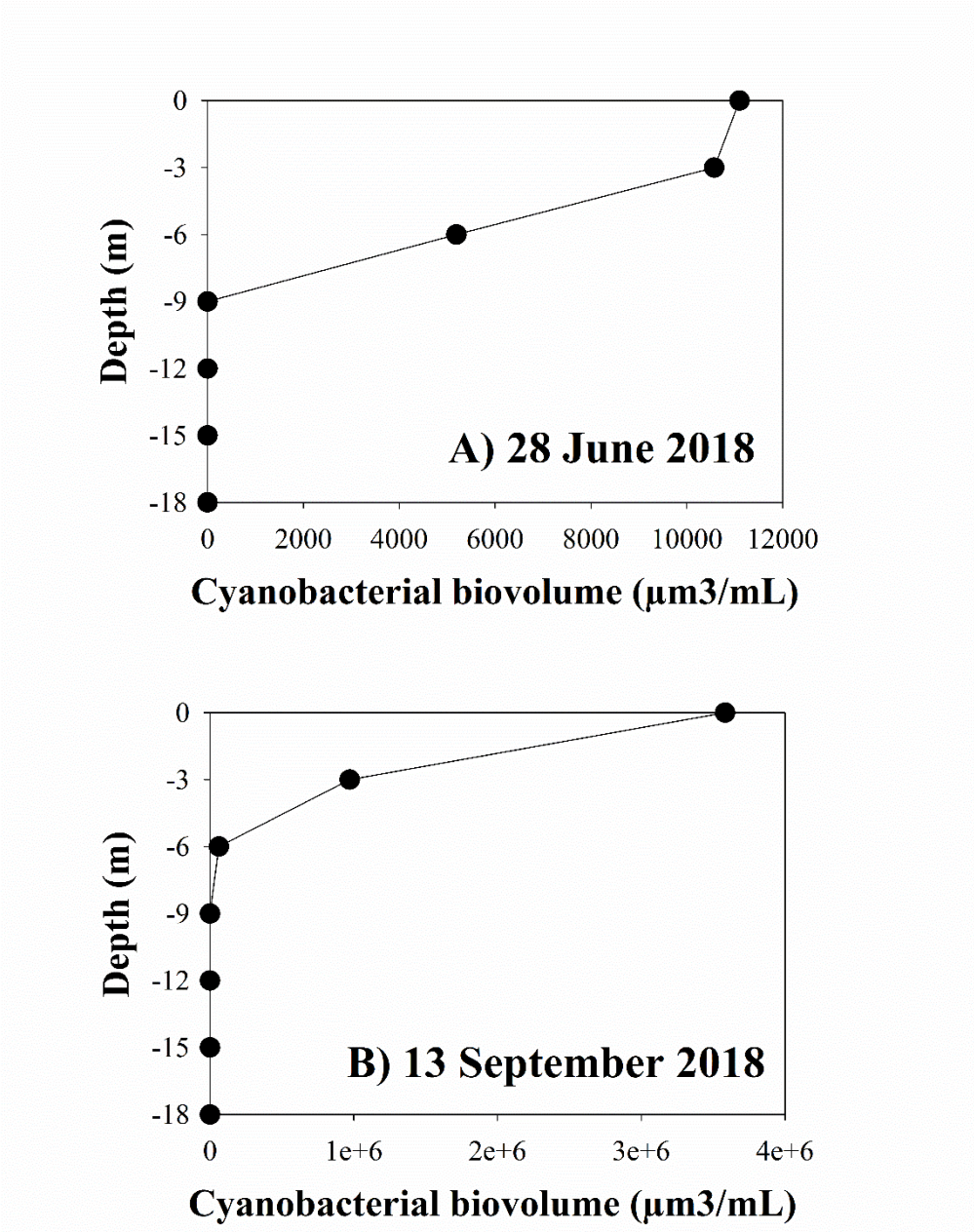

Figure 9. Depth profile of cyanobacterial biovolume for 28 June and 13 September 2018.

APPENDIX I. Hydrolab profile data.

Conesus South Data

South Station 6/13/18	Depth [m]	Temp [°C]	ORP [mV]	SpCond [µS/cm]	PAR [µE/s/m²]	LDO% [Sat]	LDO [mg/L]
	1	20.7	414	441	237	109.6	8.2
	2	20.6	415	441	134	110.2	8.3
	3	20.1	416	441	106	110.3	8.4
	4	20.1	417	440	77	109.7	8.3
	5	19.5	419	441	57	104.8	8.1
	6	16.4	431	441	41	76.8	6.3
	7	15.3	436	441	24	71.5	6.0
	8	14.1	441	440	17	63.6	5.5
	9	12.8	444	440	12	59.5	5.3
	10	12.1	446	440	9	58.1	5.2
	11	10.9	450	440	6	41.0	3.8
	12	10.8	451	440	3	40.2	3.7
	13	10.5	452	439	1	40.9	3.8
	14	10.2	453	438	1	50.2	4.7
	15	9.2	455	439	1	37.5	3.6
	16	8.8	457	438	0	30.3	3.0
	17	8.7	458	438	1	24.1	2.4
	18	8.6	251	440	1	21.9	2.1

South Station 6/21/18	Depth [m]	Temp [°C]	ORP [mV]	SpCond [µS/cm]	PAR [µE/s/m²]	LDO% [Sat]	LDO [mg/L]
	1	22.2	413	422	1601	122.6	8.9
	2	22.2	413	422	739	122.8	8.9
	3	22.1	411	422	383	122.8	9.0
	4	21.9	409	422	294	122.1	8.9
	5	21.6	408	422	161	118.8	8.8
	6	20.9	410	423	93	105.5	7.9
	7	18.8	417	424	56	85.2	6.6
	8	16.4	425	423	35	62.8	5.1
	9	14.8	429	423	22	51.0	4.3
	10	13.4	433	422	14	44.8	3.9
	11	12.1	435	421	9	39.7	3.6
	12	11.2	436	421	6	39.1	3.6
	13	11.0	437	421	5	37.2	3.4
	14	10.6	437	420	3	38.9	3.6
	15	10.1	438	419	2	40.6	3.8
	16	9.3	440	420	1	16.1	1.6
	17	8.8	442	421	1	4.0	0.4
	18	8.7	442	421	1	3.6	0.4

South Station 7/11/18	Depth [m]	Temp [°C]	ORP [mV]	SpCond [µS/cm]	PAR [µE/s/m²]	LDO% [Sat]	LDO [mg/L]
	1	25.7	417	399	1874	113.4	7.7
	2	25.8	417	399	868	114.1	7.8
	3	25.6	416	399	407	113.1	7.7
	4	25.5	415	399	175	111.3	7.6
	5	25.3	418	403	103	103.6	7.1
	6	24.0	429	412	47	65.0	4.6
	7	20.8	436	425	26	31.4	2.4
	8	18.8	438	427	14	21.3	1.7
	9	16.3	441	434	9	12.4	1.0
	10	14.6	442	432	5	10.3	0.9
	11	13.4	443	433	3	8.2	0.7
	12	12.5	445	432	2	5.3	0.5
	13	11.3	447	425	1	10.6	1.0
	14	10.9	448	424	1	11.8	1.1
	15	10.2	451	425	1	2.9	0.3
	16	9.6	417	425	1	2.6	0.3
	17	9.3	257	431	1	2.6	0.3
	18	9.1	195	434	0	2.6	0.3

South Station 7/24/18	Depth [m]	Temp [°C]	ORP [mV]	SpCond [µS/cm]	PAR [µE/s/m²]	LDO% [Sat]	LDO [mg/L]
	1	24.3	407	427	487	96.5	6.8
	2	24.3	409	427	227	96.1	6.7
	3	24.2	410	427	150	96.0	6.7
	4	24.2	411	427	87	95.8	6.7
	5	24.2	412	427	48	94.8	6.6
	6	24.2	413	427	30	94.5	6.6
	7	24.2	414	427	20	93.9	6.6
	8	18.9	430	457	11	6.0	0.5
	9	16.0	432	460	6	2.8	0.2
	10	14.1	434	458	4	2.9	0.3
	11	12.9	398	458	2	2.9	0.3
	12	12.4	275	457	2	2.9	0.3
	13	11.9	276	456	1	3.1	0.3
	14	11.4	289	454	1	4.7	0.4
	15	10.8	237	454	1	3.1	0.3
	16	10.2	198	456	1	3.1	0.3
	17	9.8	149	459	1	3.1	0.3
	18	9.7	130	460	1	3.1	0.3

South Station 7/30/18	Depth [m]	Temp [°C]	ORP [mV]	SpCond [µS/cm]	PAR [µE/s/m²]	LDO% [Sat]	LDO [mg/L]
	1	24.6	158	429	862	102.2	7.1
	2	24.6	158	429	529	102.6	7.1
	3	24.5	159	429	285	101.7	7.1
	4	24.5	160	429	188	100.7	7.0
	5	24.5	161	429	115	100.0	7.0
	6	24.5	164	429	81	95.0	6.6
	7	24.2	170	431	46	77.8	5.5
	8	19.7	184	453	24	2.6	0.2
	9	16.5	186	458	17	3.0	0.2
	10	14.4	172	460	7	2.7	0.2
	11	13.4	169	462	4	2.6	0.2
	12	12.6	170	461	3	2.7	0.2
	13	12.1	171	459	2	2.7	0.2
	14	11.6	164	457	1	2.7	0.3
	15	10.9	-	459	1	2.8	0.3
	16	10.4	-	460	1	2.8	0.3
	17	9.8	-	465	1	2.9	0.3
	18	9.6	121	466	1	2.9	0.3

South Station 8/1/18	Depth [m]	Temp [°C]	ORP [mV]	SpCond [µS/cm]	PAR [µE/s/m²]	LDO% [Sat]	LDO [mg/L]
	1	24.5	471	430	298	98.8	6.9
	2	24.5	471	431	167	98.9	6.9
	3	24.5	472	430	174	97.8	6.8
	4	24.3	474	431	89	96.0	6.7
	6	24.0	475	432	41	94.6	6.6
	6	23.9	476	432	37	86.0	6.1
	7	23.9	478	434	22	85.5	6.0
	8	17.7	491	466	17	4.4	0.4
	9	15.1	495	457	7	4.6	0.4
	10	13.6	393	461	4	2.9	0.3
	10	12.8	271	462	4	2.9	0.3
	12	12.4	244	461	2	2.9	0.3
	13	11.6	258	457	2	2.9	0.3
	14	11.4	228	456	2	2.9	0.3
	14	10.8	190	460	2	3.0	0.3
	15	10.6	163	460	1	3.0	0.3
	16	9.8	117	462	1	3.0	0.3
	17	9.6	87	464	1	3.0	0.3
	18	9.5	85	466	1	3.1	0.3
	18	9.5	82	467	1	3.1	0.3

South Station 8/10/18	Depth [m]	Temp [°C]	ORP [mV]	SpCond [µS/cm]	PAR [µE/s/m²]	LDO% [Sat]	LDO [mg/L]
	1	25.8	304	430	1155	113.0	7.7
	2	25.7	312	430	799	112.0	7.6
	3	25.7	317	431	583	111.2	7.6
	4	25.6	323	431	293	109.2	7.4
	5	25.5	327	429	208	107.4	7.4
	6	25.3	336	432	118	101.4	7.0
	7	25.1	341	432	97	93.4	6.4
	8	23.3	356	439	56	21.3	1.5
	9	20.2	359	451	41	4.4	0.3
	10	16.1	360	463	25	4.3	0.4
	11	13.9	330	466	5	3.3	0.3
	12	13.0	304	463	3	2.9	0.3
	13	12.5	266	463	2	2.8	0.3
	13	12.4	245	462	1	2.7	0.2
	14	12.0	244	461	1	2.8	0.3
	15	11.6	247	460	1	2.8	0.3
	15	10.8	147	462	1	2.8	0.3
	17	10.0	95	471	1	2.9	0.3
	18	9.8	83	472	0	2.9	0.3

South Station 8/15/18	Depth [m]	Temp [°C]	ORP [mV]	SpCond [µS/cm]	PAR [µE/s/m²]	LDO% [Sat]	LDO [mg/L]
	1	26.0	311	432	1671	109.1	7.4
	2	25.8	314	431	698	109.6	7.5
	2	25.6	315	432	699	109.6	7.5
	3	25.3	317	431	479	109.6	7.5
	4	25.3	320	432	322	106.2	7.3
	5	25.3	322	431	203	107.9	7.4
	6	25.2	325	432	130	105.7	7.3
	7	23.7	339	442	69	27.7	2.0
	8	20.7	346	454	42	5.3	0.4
	9	18.2	348	463	24	6.6	0.5
	10	15.5	350	467	7	3.2	0.3
	11	14.2	302	469	2	2.8	0.2
	12	13.1	257	468	2	2.8	0.3
	13	12.4	224	464	1	2.8	0.3
	14	11.7	210	465	1	2.9	0.3
	15	11.3	180	464	1	2.9	0.3
	16	10.5	126	470	1	2.9	0.3
	16	10.1	98	475	1	2.9	0.3
	17	10.0	88	475	1	3.0	0.3
	17	9.9	82	477	0	3.0	0.3
	18	9.8	77	477	0	3.0	0.3

South Station 8/23/18	Depth [m]	Temp [°C]	ORP [mV]	SpCond [µS/cm]	PAR [µE/s/m²]	LDO% [Sat]	LDO [mg/L]
	1	23.4	387	436	148	94.1	6.7
	2	23.4	387	435	123	92.6	6.6
	3	23.3	388	436	121	89.1	6.4
	4	23.1	390	436	81	85.7	6.1
	5	23.1	390	437	58	85.0	6.1
	6	23.1	391	436	44	84.7	6.1
	7	23.1	391	436	31	84.4	6.0
	8	23.0	391	436	21	83.0	5.9
	9	21.8	401	444	14	25.3	1.9
	10	16.3	402	467	5	3.7	0.3
	11	13.4	312	467	3	3.0	0.3
	12	12.6	239	466	1	3.1	0.3
	13	12.3	212	466	1	3.0	0.3
	14	11.8	169	468	1	3.1	0.3
	15	11.6	132	467	0	3.1	0.3
	16	10.5	108	475	1	3.2	0.3
	16	10.5	107	476	1	3.2	0.3
	18	10.0	94	479	0	3.2	0.3

South Station 9/1/18	Depth [m]	Temp [°C]	ORP [mV]	SpCond [µS/cm]	PAR [µE/s/m²]
	1	24.1	202	574	1428
	2	24.1	208	574	356
	4	24.1	212	574	145
	4	24.1	214	574	113
	5	24.1	218	574	63
	7	24.1	221	574	13
	7	24.0	222	574	21
	8	24.0	226	574	3
	8	23.7	229	576	6
	10	22.3	238	564	6
	10	19.3	240	591	9
	11	18.1	244	575	6
	11	14.7	234	609	5
	12	13.9	213	601	5
	12	13.1	187	613	2
	12	12.6	170	612	2
	13	12.9	173	605	1
	14	12.0	132	609	3
	14	12.2	135	606	1
	15	11.6	138	608	3
	15	11.3	133	610	3
	16	10.8	125	619	4
	16	10.6	116	620	4
	16	10.6	110	616	2
	17	10.0	96	622	1
	18	10.0	102	623	1

South Station 9/27/18	Depth [m]	Temp [°C]	ORP [mV]	SpCond [µS/cm]	PAR [µE/s/m²]	LDO% [Sat]	LDO [mg/L]
	1	21.1	264	584	246	104.1	9.2
	1	21.1	266	584	146	104.0	9.2
	2	20.8	272	585	37	102.4	9.2
	3	20.6	276	585	17	93.1	8.4
	4	20.5	279	586	7	87.2	7.8
	5	20.5	281	586	3	85.1	7.7
	6	20.5	282	585	1	84.8	7.6
	7	20.5	283	585	1	84.4	7.6
	8	20.5	284	585	0	83.6	7.5
	9	20.5	285	585	0	83.5	7.5
	9	20.4	286	585	0	83.4	7.5
	11	19.8	291	592	0	49.9	4.6
	11	18.9	295	599	1	28.1	2.6
	12	16.9	282	615	0	6.2	0.6
	13	14.6	178	627	0	5.1	0.5
	14	13.1	130	625	0	4.5	0.5
	15	11.9	116	629	0	4.5	0.5
	16	10.9	101	641	1	4.4	0.5
	17	10.7	94	641	1	4.4	0.5
	18	10.5	89	643	0	4.4	0.5

Conesus Center Data

Center Station 6/13/18	Depth [m]	Temp [°C]	ORP [mV]	SpCond [µS/cm]	PAR [µE/s/m²]	LDO% [Sat]	LDO [mg/L]
	1	20.1	451	441	281	107.5	8.2
	2	20.1	449	441	187	107.5	8.2
	3	20.2	447	441	105	107.8	8.2
	4	20.1	446	441	71	107.6	8.2
	5	20.2	444	441	44	107.4	8.1
	6	20.1	444	441	25	106.9	8.1
	7	20.1	444	441	13	106.2	8.1
	8	19.5	445	441	9	104.2	8.0
	8	19.2	447	440	10	99.3	7.7
	8	19.5	446	441	14	102.8	7.9
	9	17.2	454	441	10	75.1	6.1
	10	15.3	461	442	9	60.6	5.1
	11	11.9	468	441	4	37.0	3.4

Center Station 6/21/18	Depth [m]	Temp [°C]	ORP [mV]	SpCond [µS/cm]	PAR [µE/s/m²]	LDO% [Sat]	LDO [mg/L]
	1	22.4	372	414	1428	117.3	8.5
	2	22.4	372	421	797	121.7	8.8
	3	22.3	374	422	454	122.0	8.9
	4	22.0	377	421	252	118.4	8.6
	5	21.6	381	422	169	110.9	8.2
	6	20.3	387	426	102	95.4	7.2
	7	19.2	391	424	59	89.8	6.9
	8	17.8	398	425	36	72.0	5.7
	9	15.6	405	424	22	55.6	4.6
	10	13.1	410	422	14	38.9	3.4
	11	12.1	411	422	9	32.8	3.0
	12	10.8	414	422	5	25.9	2.4

Center Station 7/5/18	Depth [m]	Temp [°C]	ORP [mV]	SpCond [µS/cm]	PAR [µE/s/m²]	LDO% [Sat]	LDO [mg/L]
	1	27.8	388	405	577	128.8	8.4
	1	27.7	387	405	366	129.1	8.5
	2	27.5	389	406	163	129.7	8.5
	2	27.6	389	405	165	129.7	8.5
	2	27.6	389	404	165	129.6	8.5
	3	27.2	391	406	82	129.1	8.6
	4	26.7	393	405	34	128.6	8.6
	5	25.8	396	410	18	122.1	8.3
	6	22.8	401	419	8	99.6	7.2
	7	21.4	405	423	4	80.0	5.9
	8	19.2	411	423	2	52.2	4.0
	8	19.9	413	423	5	39.5	3.0
	9	17.3	417	426	3	30.0	2.4
	10	14.2	420	428	2	18.5	1.6
	11	12.6	422	427	1	8.9	0.8
	12	11.6	423	425	1	5.4	0.5
	12	11.2	424	425	1	4.4	0.4
	13	10.9	425	423	1	3.9	0.4

Center Station 7/11/18	Depth [m]	Temp [°C]	ORP [mV]	SpCond [µS/cm]	PAR [µE/s/m²]	LDO% [Sat]	LDO [mg/L]
	1	25.8	391	399	1242	109.5	7.4
	1	25.8	399	399	2377	109.9	7.5
	2	25.7	392	400	717	110.6	7.5
	3	25.7	395	399	343	109.9	7.5
	4	25.4	404	401	145	95.7	6.6
	5	24.0	416	411	73	64.4	4.5
	6	22.4	421	420	41	39.1	2.8
	7	21.3	424	422	20	30.8	2.3
	8	20.2	425	425	12	26.4	2.0
	9	17.2	427	430	6	16.0	1.3
	10	16.3	428	432	4	13.3	1.1
	10	15.5	430	428	4	11.0	0.9
	11	11.6	434	430	2	2.8	0.3
	12	11.4	435	429	1	2.6	0.2

Center Station 7/16/18	Depth [m]	Temp [°C]	ORP [mV]	SpCond [µS/cm]	PAR [µE/s/m²]	LDO% [Sat]	LDO [mg/L]
	0	27.5	356	398	264	140.8	9.3
	1	27.4	361	398	89	141.7	9.4
	2	27.1	365	398	48	141.5	9.4
	3	26.6	368	398	25	140.1	9.4
	4	26.1	374	400	15	123.4	8.4
	5	25.6	380	401	9	109.6	7.5
	6	24.4	392	409	5	71.2	5.0
	7	23.1	399	417	3	44.7	3.2
	8	18.5	403	431	2	10.8	0.9
	9	16.0	405	434	2	5.4	0.5
	9	15.2	404	438	1	4.8	0.4
	10	14.4	405	431	1	4.4	0.4
	11	12.9	406	432	1	3.7	0.3
	11	11.7	370	431	1	2.9	0.3
	12	11.6	325	432	0	2.9	0.3

Center Station 7/21/18	Depth [m]	Temp [°C]	ORP [mV]	SpCond [µS/cm]	PAR [µE/s/m²]	LDO% [Sat]	LDO [mg/L]
	1	25.4	329	425	480	109.3	7.5
	2	25.4	334	424	188	109.7	7.5
	2	25.4	337	424	133	109.9	7.5
	3	25.4	340	424	104	110.3	7.6
	3	25.4	340	424	114	110.6	7.6
	4	25.4	342	422	69	109.3	7.5
	4	25.4	343	421	63	109.4	7.5
	5	25.4	345	421	52	109.3	7.5
	6	25.4	348	421	35	109.1	7.5
	7	25.4	350	420	21	108.7	7.5
	8	25.3	352	420	17	107.5	7.4
	8	25.3	358	420	12	105.8	7.3
	8	25.0	363	421	13	88.7	6.1
	10	16.3	370	461	8	4.2	0.3
	11	12.8	301	452	3	2.9	0.3
	13	11.1	218	450	1	3.0	0.3

Center Station 7/24/18	Depth [m]	Temp [°C]	ORP [mV]	SpCond [µS/cm]	PAR [µE/s/m²]	LDO% [Sat]	LDO [mg/L]
	1	24.6	372	424	158	102.6	7.1
	2	24.6	374	425	143	102.1	7.1
	3	24.6	376	425	102	100.7	7.0
	4	24.6	378	425	62	99.6	6.9
	5	24.6	380	425	43	99.3	6.9
	6	24.5	382	423	27	97.1	6.8
	7	24.4	385	423	17	94.1	6.6
	8	21.7	399	441	10	28.8	2.1
	9	18.7	403	452	7	6.2	0.5
	10	16.3	405	455	4	3.0	0.2
	11	12.2	239	454	2	3.0	0.3
	12	12.1	191	454	1	3.0	0.3

Center Station 7/30/18	Depth [m]	Temp [°C]	ORP [mV]	SpCond [µS/cm]	PAR [µE/s/m²]	LDO% [Sat]	LDO [mg/L]
	1	24.8	102	425	367	101.8	7.0
	2	24.7	106	425	227	100.7	7.0
	3	24.7	109	425	139	100.1	6.9
	4	24.7	113	425	89	99.3	6.9
	5	24.6	118	426	55	91.4	6.4
	6	24.1	131	432	34	67.9	4.8
	7	23.3	141	437	21	39.1	2.8
	8	22.0	148	443	14	13.6	1.0
	9	18.0	150	459	9	2.6	0.2
	10	15.5	152	461	6	2.6	0.2
	11	14.2	109	463	2	2.6	0.2
	12	12.9	-11	463	1	2.6	0.2

Center Station 8/1/18	Depth [m]	Temp [°C]	ORP [mV]	SpCond [µS/cm]	PAR [µE/s/m²]	LDO% [Sat]	LDO [mg/L]
	1	24.7	344	429	489	104.5	7.3
	2	24.7	349	428	326	103.7	7.2
	3	24.6	357	428	171	102.7	7.1
	4	24.6	361	428	115	102.6	7.1
	5	24.6	365	429	63	100.0	7.0
	6	24.5	369	428	42	100.0	7.0
	7	24.5	371	429	25	99.9	7.0
	8	24.5	374	429	17	98.6	6.9
	9	24.4	379	429	11	96.1	6.7
	9	24.5	380	429	12	91.7	6.4
	9	24.4	383	429	10	89.2	6.2
	10	21.0	392	450	8	7.2	0.5
	10	24.3	384	430	8	80.2	5.6
	10	23.4	394	436	7	43.4	3.1
	10	21.5	400	447	7	6.1	0.5
	11	16.8	394	460	4	3.7	0.3
	12	13.6	149	465	2	2.8	0.2

Center Station 8/10/18	Depth [m]	Temp [°C]	ORP [mV]	SpCond [µS/cm]	PAR [µE/s/m²]	LDO% [Sat]	LDO [mg/L]
	1	25.8	292	427	166	108.2	7.4
	2	25.8	287	426	165	108.1	7.4
	3	25.8	279	426	108	107.3	7.3
	4	25.7	271	427	70	107.1	7.3
	5	25.7	254	427	50	98.8	6.7
	6	25.2	239	431	33	79.1	5.4
	7	24.2	220	434	21	49.6	3.5
	8	22.4	194	441	15	20.9	1.5
	9	20.0	173	452	9	6.5	0.5
	9	15.9	147	462	5	2.5	0.2
	10	13.6	129	466	1	2.7	0.2
	12	11.8	125	462	1	2.8	0.3

Center Station 8/15/18	Depth [m]	Temp [°C]	ORP [mV]	SpCond [µS/cm]	PAR [µE/s/m²]	LDO% [Sat]	LDO [mg/L]
	1	25.2	414	430	1720	101.3	7.0
	1	25.1	414	430	1082	102.0	7.0
	1	25.0	397	431	2179	87.6	6.1
	2	25.0	415	430	806	101.1	7.0
	3	24.9	416	431	430	99.8	6.9
	4	24.9	417	430	241	99.2	6.9
	5	24.9	418	431	135	96.3	6.7
	6	24.8	419	431	86	93.7	6.5
	7	24.6	423	432	60	80.3	5.6
	8	24.3	427	434	40	67.9	4.8
	8	22.1	416	447	29	9.5	0.7
	9	18.4	425	459	21	4.1	0.3
	10	16.7	401	462	6	2.8	0.2
	11	13.7	213	467	3	2.8	0.3
	12	12.2	149	468	2	2.9	0.3
	13	12.0	126	468	1	2.9	0.3

Center Station 8/23/18	Depth [m]	Temp [°C]	ORP [mV]	SpCond [µS/cm]	PAR [µE/s/m²]	LDO% [Sat]	LDO [mg/L]
	1	23.8	317	433	318		
	2	23.6	318	433	122		
	3	23.6	319	433	93		
	4	23.3	323	434	74		
	5	23.2	325	434	59		
	6	23.2	327	435	44		
	7	23.0	330	436	30		
	8	22.7	335	440	21		
	9	22.2	341	445	5		
	10	18.5	346	457	5		
	11	15.8	257	464	2		
	12	12.2	91	515	1		

Center Station 9/1/18	Depth [m]	Temp [°C]	ORP [mV]	SpCond [µS/cm]	PAR [µE/s/m²]
	1	24.2	314	576	932
	2	24.2	314	576	580
	3	24.2	315	576	320
	4	24.1	316	576	190
	5	23.9	318	577	104
	6	23.8	320	577	61
	7	23.7	322	577	39
	8	23.3	326	575	23
	9	22.2	333	581	17
	9	21.7	335	581	13
	9	21.7	336	582	13
	10	20.1	339	588	9
	11	18.8	341	595	6
	11	18.6	344	595	5
	12	15.3	141	612	3
	13	15.0	148	613	3
	13	14.8	133	613	3
	13	14.8	127	613	3

Center Station 9/27/18	Depth [m]	Temp [°C]	ORP [mV]	SpCond [µS/cm]	PAR [µE/s/m²]	LDO% [Sat]	LDO [mg/L]
	0	21.3	271	580	273	110.3	9.8
	1	21.4	273	582	166	106.5	9.4
	2	21.0	277	579	65	105.3	9.4
	3	20.9	280	580	31	98.4	8.8
	4	20.9	284	580	13	88.9	7.9
	5	20.9	286	580	6	88.5	7.9
	6	20.9	288	580	3	86.0	7.7
	7	20.8	290	581	1	86.0	7.7
	8	20.7	292	583	1	84.7	7.6
	9	20.3	295	588	1	83.3	7.5
	10	20.0	298	590	0	71.8	6.5
	10	20.0	302	591	0	50.2	4.6
	10	19.9	303	592	1	53.7	4.9
	12	18.9	306	598	0	32.1	3.0
	13	13.5	131	631	0	5.7	0.6
	13	13.3	117	632	1	4.9	0.5

APPENDIX II.

Survey of Adult Dreissenid Mussel Populations in Conesus Lake New York

INTRODUCTION

Zebra mussels colonized the Great Lakes system in 1984 and by 1992 they had dispersed into Conesus Lake. In the 1990's the Eurasian quagga mussel (*D. rostriformis bugensis*), colonized North America and supplemented or largely replaced zebra mussels in temperate lakes. Because they feed at similar size-dependent rates and exhibit some of same rejection mechanisms as zebra mussels, quagga mussels are expected to intensify the threat of *Microcystis* and cyanobacterial blooms (Tang et al., 2013).

Zebra mussels were first seen in Conesus Lake in 1992. By 1994, juvenile settlement had increased in the southern region of the lake and by 1998 adult populations were established throughout Conesus Lake and had already caused considerable loss in unionid mussel populations (IB personal observations). The first major survey of adult populations in Conesus Lake was conducted in 2000 (Bosch et al, 2001). Population numbers were relatively high at an $27.8x10^3 \cdot m^{-2}$ and median of $27.3x10^3 \cdot m^{-2}$. Most of the materials collected were living mussels and shell debris was minimal along the bottom. A second survey conducted in 2013 at the very same sites visited in 2000 produced a very different impression of the fate of these populations. Average population numbers were at $13.0\ x10^3 \cdot m^{-2}$ and median values were $9.2x10^3 \cdot m^{-2.}$ (Bosch et al., 2013). No quagga mussels were identified among more than 750 adult mussels from different sites that were examined for that study. One of the goals of this summer's monitoring is to determine whether quagga mussels have colonized Conesus Lake since 2013.

METHODS

Collections were all made on August 9, 2018 using a Petersen Grab dredge. This mode of collection method could not be used to quantify mussel abundance. The two previous surveys in Conesus Lake were carried out by SCUBA divers.

Samples were taken from 4, 8, and 10 m depths. The sites surveyed were Pebble Beach, Grayshores, Eagle Point and Sand Point. We tried to sample at McPherson's Cove, Cottonwood Gully and North Sutton Point where we had sampled before but high amounts of macrophytes or sediment, or shell debris impeded our collections.

At leat 50 animals were counted for site/depth and more than 550 were counted in total. We relied on shell morphology to distinguish zebra mussels from quagga mussels. Overall, quagga mussels are more spatulate, while zebra mussels have a more lancelate shape. The ventral portion of the zebra mussel shell is flattened, and there is a definite angle between the ventral and dorsal surfaces, whreas the quagga has a more rounded ventral end and the ventralside is convex (USGS Nonindigious Species Web Site). These differences are widely used to distinguish the two species and the method seems to be generally reliable and widely accepted in the scientific literature.

RESULTS AND DISCUSSION

We inspected more than 500 mussels combined from the 4 sites where we collected and all were all zebra mussels, *Dreissena polymorpha*. Photographs of some of the individuals collected are shown in **Figure A1**. While we could not obtain abundance counts with the collection method used, it was apparent that the population numbers in the area sampled were low. Often it took several Grab collections to obtain the threshold of 50 mussels that we wanted for each location. Most of the material that came up was shell debris. Our anecdotal observation is that the populations are even lower than what we observed in 2013, when they had already declined significantly since the peak abundance reported in 2001. **Figure A2** shows the size frequency distribution of species for the sites sampled. We could not see any important differences between these size frequency distributions and the ones previously reported by Bosch and colleagues in 2001 and 2013. All three years seem to indicate that there is a low rate of recruitment toward the typical adult size.

We conclude that quagga mussels are either not present in Conesus Lake or not present in significant to be detected by our sample size. Although we did not conduct quantitative surveys of abundance, our observation is that zebra mussels are not as abundant as they were in previous surveys. It is not clear why this trend continues. As reported earlier in this paper, there seems to have been no significant change in the trophic state index of Conesus Lake since 2004. This index takes into account chlorophyll *a* and water clarity, two factors that affect and are changed by the presence of significant zebra mussel populations.

Figure A1. Photographs of mussels collected for this study, all of which were inspected and identified as zebra mussels and not quagga mussels.

Figure A2. Size frequency distributions of mussels from different locations combined. Sample size was at least 50 mussels for each site.